

# CURRENT STATUS OF THE HIGH-REPETITION-RATE ELECTRON DRIVEN PULSED MUON SOURCE AT THE SHINE FACILITY

J. K. Ng\*, J. C. Yap, K. S. Khaw

Tsung-Dao Lee Institute and School of Physics and Astronomy,  
Shanghai Jiao Tong University, Shanghai, China

## Abstract

Shanghai High-repetition-rate XFEL and Extreme Light (SHINE) Facility provides an 8 GeV, 1 MHz, 100 pC electron beam, offers a unique driver for an electron-driven muon source complementary to existing proton-based facilities. Simulation studies have demonstrated the potential of such a source for muon-based fundamental physics and applied research. Realization of this type of muon beamline presents challenges, including lower per-bunch yield, high background, and the need for new measurement methods. As a first step, we propose a feasibility study of a muon yield measurement at SHINE facility using a compact vacuum chamber with scintillator detectors. The measurement strategy is validated through end-to-end simulation incorporating optical photon process and realistic photodetector response, demonstrating that muon decay signal can be isolated from the mixed secondary beam.

## INTRODUCTION

Muons play an increasingly important role in fundamental physics and applied sciences, for example: precision test of the Standard Model [1], searches for physics beyond the Standard Model [2], muon spin rotation ( $\mu$ SR) [3], and many more. Many such experiments are statistically limited by the time structure of existing proton-driven sources: current facilities operate either in pulsed mode at 25–50 Hz (e.g., J-PARC [4]) or in continuous mode (e.g., PSI [5]), while optimal statistical performance requires repetition rates in the tens of kilohertz range [6–10].

Several alternatives have been proposed in order to achieve a high-repetition-rate driver for muon production, including attempts on proton accelerators [11, 12]. Muon production via electron-beam-induced photonuclear process in a fixed target offers another alternative independent from proton accelerators [13]. This is of particular interest as the production scheme can be implemented at existing XFEL facility, as well as laser wakefield acceleration facilities [14]. For example, the Shanghai High-repetition-rate XFEL and Extreme Light (SHINE) Facility [15] capable of delivering 100 pC electron bunches at 8 GeV, 1 MHz, is a promising driver for such a source. Initial feasibility studies [16] and subsequent detailed target and beamline simulations [17] demonstrated competitive surface muon rates with an ideal time structure and high polarisation.

Transitioning from simulation to experiment presents significant challenges: low per-bunch yield, intense mixed

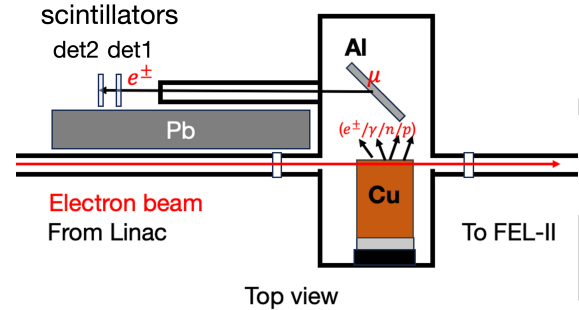


Figure 1: Schematic of the beam test setup. A Cu production target converts the 3 GeV electron beam into a mixed secondary beam; an Al stopping target ranges out surface muons; two plastic scintillators with SiPM readout detect muon decay positrons for lifetime analysis.

secondary background ( $e^\pm$ ,  $\gamma$ , hadrons), and no event-by-event particle tagging. This paper reports the current status of our preparation towards a beam test at SHINE FEL-II (Shaft #2), including detector development, an end-to-end Geant4-based simulation framework, and background characterisation studies that validate the measurement strategy.

## BEAM TEST SETUP AT SHINE

The beam test is planned at SHINE FEL-II, Shaft #2, using a 3 GeV electron beam at 10–100 Hz with 50–100 pC per bunch. A compact vacuum chamber houses the complete production and detection chain. Electrons impinge on a copper (Cu) production target, generating a mixed secondary beam comprising muons, pions, electrons, positrons, photons, and neutrons. The secondary beam traverses an aluminium (Al) stopping target sized to range out surface muons ( $p \approx 29.8$  MeV/c), stopped  $\mu^+$  then decay via  $\mu^+ \rightarrow e^+ \nu_e \bar{\nu}_\mu$  (see Fig. 1).

Two plastic scintillators with silicon photomultiplier (SiPM) readout detect the muon decay positrons downstream of the stopping target: Detector 1 (near) and Detector 2 (far). Each scintillator is instrumented with two SiPMs read out in coincidence. The SiPM waveforms in the 24  $\mu$ s-time window after an accelerator trigger event are digitised by a PicoScope (Pico Technology, UK) DAQ system at a time resolution of 4 ns, and a ADC resolution of 8-bit.

Prior to measurement, the DAQ and analysis pipeline were validated using cosmic muons, demonstrating that the system correctly measures the muon lifetime in a clean single-muon decay scenario.

\* ngjunkai@sjtu.edu.cn

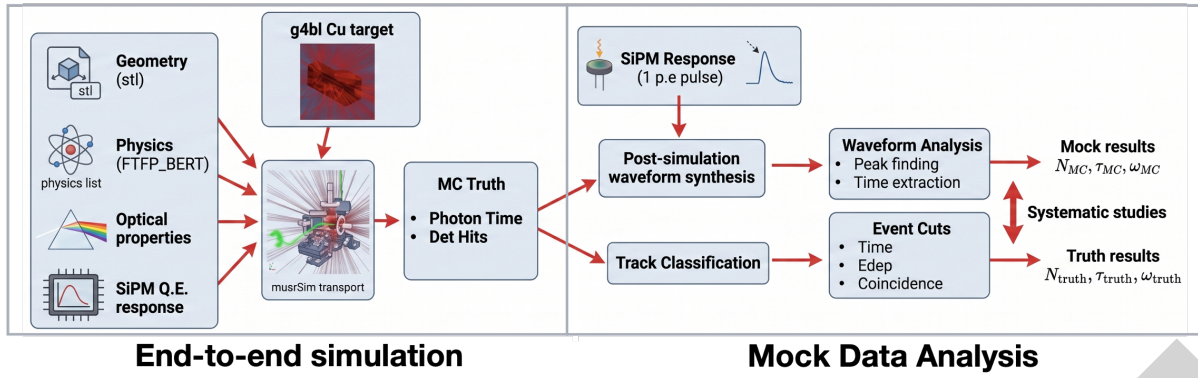


Figure 2: End-to-end simulation pipeline. G4BL and musrSim generate the same event data; two parallel analysis tracks—truth (particle-level ROOT trees) and waveform synthesis (mimicking realistic SiPM response and digitization)—run on the same simulated output.

## END-TO-END SIMULATION FRAMEWORK

The simulation is built around two sequential stages. `g4beamline` (with `QGSP_BERT` physics list) [18] models primary beam transport through the Cu production target and generates the secondary particle kinematics. The secondary beam is then passed to `musrSim` [19]—a `Geant4`-based [20] package developed at PSI and widely used in  $\mu$ SR detector simulation—which models the full detector geometry, employs the `FTFP_BERT` physics list, and includes optical photon transport. A measured SiPM response was also imported to the simulation.

Two parallel analysis tracks are applied to the same simulated dataset, as illustrated in Fig. 2. The *truth analysis* reads particle-level ROOT [21] trees directly, giving access to the PDG identity, production process, time, and energy deposition of every track in each scintillator. The *waveform analysis* synthesises detector waveforms from the simulated optical photon arrival times, mimicking the realistic SiPM readout, and analyses these waveforms with the same algorithms that will be applied to beam data.

Agreement between the two tracks validates the analysis pipeline. Disagreement identifies analysis-level systematics that must be understood before beam data are taken. As a benchmark, all three estimates agree with the PDG muon lifetime of 2197 ns [22] within 10%: cosmic muons  $\tau = 2.078 \pm 0.133 \mu\text{s}$ , truth analysis  $\tau = 2080 \pm 53 \text{ ns}$ , and waveform analysis  $\tau = 2.191 \pm 0.006 \mu\text{s}$ , validating the end-to-end measurement chain.

## BACKGROUND CHARACTERISATION AND SIGNAL EXTRACTION

### Background Event Topology

In the truth analysis, secondary particles are classified by PDG identity and `Geant4` production process. Three categories are observed in the scintillators after a  $1 \mu\text{s}$  time gate (which suppresses the prompt flash from beam-synchronous particles):

- **Signal:** positrons from  $\mu^+$  decay at rest,  $\mu^+ \rightarrow e^+ \nu_e \bar{\nu}_\mu$  (Michel positrons), selected by `PDGID = -11` (positron) and `process = DecayWithSpin`. The stopped-muon interpretation is supported by the single-exponential time spectrum with  $\tau = 2080 \pm 53 \text{ ns}$ , in the range of the free-muon lifetime [22]; a significant in-flight component would distort the spectrum and bias  $\tau$  high.
- **Hadronic background:** primarily neutrons from  $\mu^-$  nuclear capture and hadronic cascade reactions. These exhibit a two-component time structure and are statistically exhausted by  $\sim 10 \mu\text{s}$ .
- **Electromagnetic (EM) background:**  $e^\pm$  consistent with originating from the  $\mu^+$  decay chain—these follow the same exponential time distribution as the signal and are therefore indistinguishable in the time domain alone.

Without background rejection, the signal yield is overestimated by a factor of 4.6.

### Energy Deposition Cut

A minimum energy deposition threshold of 0.1 MeV is applied independently to each detector entry. Neutrons deposit far less than 0.1 MeV in plastic scintillator via elastic scattering, so this cut removes the entire hadronic background. EM tracks mostly clear the threshold and survive (see Fig. 3).

Crucially, the cut is applied per detector (not on the summed `Edep`), matching the physical AND logic of the SiPM readout: each SiPM pair fires independently, and a track invisible to one detector is invisible regardless of what the other sees.

Fitting the surviving event sample with an exponential confirms that the EM background does not bias the lifetime measurement:  $\tau_{\text{bkg}} = 2127 \pm 51 \text{ ns}$  versus  $\tau_{\text{sig}} = 2080 \pm 53 \text{ ns}$ , a difference of  $0.65 \sigma$ . The  $\tau$  extraction is therefore unbiased; the contamination affects only the absolute yield (see Fig. 4).

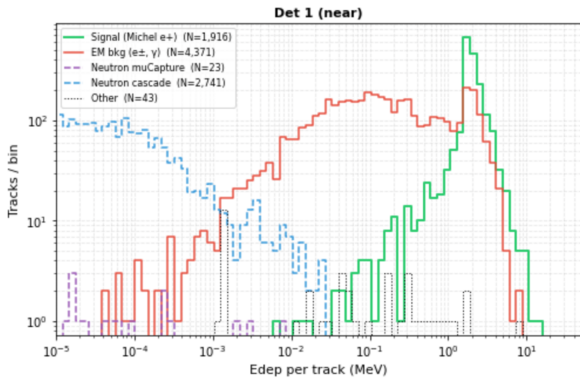


Figure 3: Energy deposition distribution per track in Detector 1. Neutrons (hadronic background) deposit well below 0.1 MeV, while signal (Michel  $e^+$ ) and EM background are concentrated above this threshold, motivating the Edep cut.

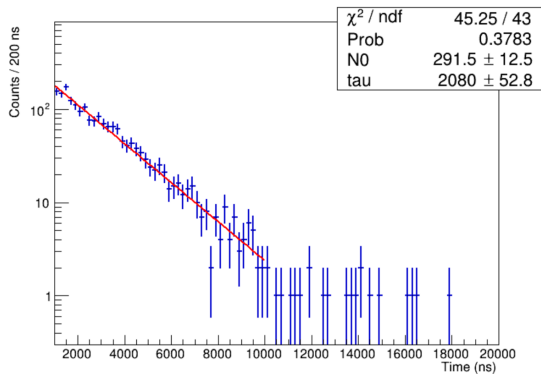


Figure 4: Decay time spectrum of signal tracks in Detector 1 after the Edep cut, with a single exponential fit.

### Detector Coincidence

After the Edep cut the residual background is purely electromagnetic. Most EM tracks are single-detector events: low-energy  $e^\pm$  in the EM background range out or convert before reaching Detector 2. Requiring a *coincidence*—both Detector 1 and Detector 2 each independently exceeding the 0.1 MeV threshold—selects through-going tracks and preferentially rejects single-detector EM events.

The coincidence requirement reduces signal yield by approximately half: roughly half of all Michel positrons have energies low enough to stop before Detector 2, consistent with the Michel endpoint of 52.83 MeV. The time difference  $\Delta t$  between the two detectors is consistent with zero for all genuine through-going tracks, confirming that a coincidence time window of  $\leq 2$  ns is sufficient.

Under the combined Edep cut and coincidence requirement, the signal survival fraction is 45.4%, the background survival fraction is 4.3%, and the resulting sample purity is 73.5%. The 0.1 MeV threshold used here is a conservative placeholder; a calibrated threshold will be established once the Edep-to-waveform conversion is determined from an independent calibration with known sources.

## SUMMARY AND FUTURE WORK

We have developed an end-to-end simulation framework for the feasibility study of a muon yield measurement at the SHINE facility. The DAQ and analysis chain were first validated in a clean single-muon scenario using cosmic muons. For the more complex beam environment—multiple particle species, high background—the waveform synthesis pipeline, incorporating optical photon transport and realistic photodetector response, is validated by agreement with the truth analysis, confirming that the detection scheme is expected to work under beam conditions.

Background characterisation reveals two distinct populations: hadronic (removed by a per-detector energy deposition cut) and electromagnetic (suppressed by detector coincidence). The combined cuts achieve 73.5% sample purity with an unbiased lifetime extraction, providing a basis for further understanding of systematic effects before beam data are acquired.

Future work will focus on: (1) absolute muon yield extraction; (2) feasibility study for muon polarisation measurement; and (3) measurement with beam at SHINE FEL-II.

## ACKNOWLEDGEMENTS

We are grateful to Yu Bao, Vadim Grinenko, Hong Ding, Bo Liu, Zhi Liu, Jian Tang, Dao Xiang, and Zhentang Zhao for fruitful discussions regarding the beamline optimization and physics potential of the SHINE muon beam. The work is supported by the Shanghai Pilot Program for Basic Research (Grant No. 21TQ1400221).

## REFERENCES

- [1] T. P. Gorringer and D. W. Hertzog, “Precision muon physics”, *Prog. Part. Nucl. Phys.*, vol. 84, pp. 73–123, 2015. [doi:10.1016/j.pnpnp.2015.06.001](https://doi.org/10.1016/j.pnpnp.2015.06.001)
- [2] Y. Kuno and Y. Okada, “Muon decay and physics beyond the standard model”, *Rev. Mod. Phys.*, vol. 73, no. 1, pp. 151–202, Jan. 2001. [doi:10.1103/RevModPhys.73.151](https://doi.org/10.1103/RevModPhys.73.151)
- [3] A. D. Hillier *et al.*, “Muon spin spectroscopy”, *Nature Reviews Methods Primers*, vol. 2, no. 1, p. 4, Jan. 2022. [doi:10.1038/s43586-021-00089-0](https://doi.org/10.1038/s43586-021-00089-0)
- [4] Y. Miyake *et al.*, “Current status of the J-PARC muon facility, MUSE”, *J. Phys. Conf. Ser.*, vol. 551, no. 1, p. 012061, 2014. [doi:10.1088/1742-6596/551/1/012061](https://doi.org/10.1088/1742-6596/551/1/012061)
- [5] J. Grillenberger, C. Baumgarten, and M. Seidel, “The High Intensity Proton Accelerator Facility”, *SciPost Phys. Proc.*, no. 5, p. 002, 2021. [doi:10.21468/scipostphysproc.5.002](https://doi.org/10.21468/scipostphysproc.5.002)
- [6] R. Cywinski *et al.*, “Towards a dedicated high-intensity muon facility”, *Physica B*, vol. 404, pp. 1024–1027, 2009. [doi:10.1016/j.physb.2008.11.203](https://doi.org/10.1016/j.physb.2008.11.203)
- [7] S. Kanda, “Toward a high-precision measurement of the muon lifetime with an intense pulsed muon beam at J-PARC”, in *Proc. NuFact2021*, Cagliari, Italy, Sep. 2021, p. 215. [doi:10.22323/1.402.0215](https://doi.org/10.22323/1.402.0215)

- [8] A. Adelmann, K. Kirch, C. J. G. Onderwater, and T. Schietinger, “Compact storage ring to search for the muon electric dipole moment”, *J. Phys. G*, vol. 37, p. 085001, 2010.  
[doi:10.1088/0954-3899/37/8/085001](https://doi.org/10.1088/0954-3899/37/8/085001)
- [9] L. Willmann and K. Jungmann, “Muonium-antimuonium conversion”, *SciPost Phys. Proc.*, vol. 5, p. 009, 2021.  
[doi:10.21468/SciPostPhysProc.5.009](https://doi.org/10.21468/SciPostPhysProc.5.009)
- [10] Y. Ema, T. Gao, and M. Pospelov, “Muon spin force”, *Phys. Rev. D*, vol. 110, no. 7, p. 075024, Oct. 2024.  
[doi:10.1103/PhysRevD.110.075024](https://doi.org/10.1103/PhysRevD.110.075024)
- [11] L. Bartoszek *et al.*, “Mu2e Technical Design Report”, Oct. 2014. [doi:10.2172/1172555](https://doi.org/10.2172/1172555)
- [12] Y. Liu, A. Rakhman, C. D. Long, Y. Liu, and T. J. Williams, “Laser-assisted high-energy proton pulse extraction for feasibility study of co-located muon source at the SNS”, *Nucl. Instrum. Meth. A*, vol. 962, p. 163706, 2020.  
[doi:10.1016/j.nima.2020.163706](https://doi.org/10.1016/j.nima.2020.163706)
- [13] K. Nagamine, H. Miyadera, A. Jason, and R. Seki, “Compact muon source with electron accelerator for a mobile mu SR facility”, *Physica B*, vol. 404, pp. 1020–1023, 2009.  
[doi:10.1016/j.physb.2008.11.231](https://doi.org/10.1016/j.physb.2008.11.231)
- [14] F. Zhang *et al.*, “Proof-of-principle demonstration of muon production with an ultrashort high-intensity laser”, *Nature Phys.*, vol. 21, no. 7, pp. 1050–1056, 2025.  
[doi:10.1038/s41567-025-02872-2](https://doi.org/10.1038/s41567-025-02872-2)
- [15] Z. Zhu, Z. T. Zhao, D. Wang, Z. H. Yang, and L. Yin, “SCLF: An 8-GeV CW SCRF linac-based X-ray FEL facility in Shanghai”, in *Proc. FEL'17*, Santa Fe, NM, USA, Aug. 2017, pp. 182–184. [doi:10.18429/JACoW-FEL2017-MOP055](https://doi.org/10.18429/JACoW-FEL2017-MOP055)
- [16] M. Lv, J. Wang, and K. S. Khaw, “A pulsed muon source based on a high-repetition-rate electron accelerator”, in *Proc. IPAC'23*, Venice, Italy, pp. 1522–1525, Sep. 2023.  
[doi:10.18429/JACoW-IPAC2023-TUPA087](https://doi.org/10.18429/JACoW-IPAC2023-TUPA087)
- [17] Y. Takeuchi, K. S. Khaw, F. Liu, J. K. Ng, and J. Wang, “Design studies on a kHz–MHz repetition rate pulsed muon source based on electron accelerator”, in *Proc. IPAC'25*, Taipei, Taiwan, pp. 1372–1375, Nov. 2025.  
[doi:10.18429/JACoW-IPAC2025-TUPM092](https://doi.org/10.18429/JACoW-IPAC2025-TUPM092)
- [18] T. J. Roberts and D. M. Kaplan, “G4Beamline Simulation Program for Matter Dominated Beamlines”, *Conf. Proc. C*, vol. 070625, p. 3468, 2007.  
[doi:10.1109/PAC.2007.4440461](https://doi.org/10.1109/PAC.2007.4440461)
- [19] K. Sedlak, R. Scheuermann, T. Shiroka, A. Stoykov, A. R. Raselli, and A. Amato, “musrSim and musrSimAna – simulation tools for  $\mu$ SR instruments”, *Phys. Proc.*, vol. 30, pp. 61–64, 2012. [doi:10.1016/j.phpro.2012.04.040](https://doi.org/10.1016/j.phpro.2012.04.040)
- [20] S. Agostinelli *et al.*, “GEANT4 - a simulation toolkit”, *Nucl. Instrum. Meth. A*, vol. 506, pp. 250–303, 2003.  
[doi:10.1016/S0168-9002\(03\)01368-8](https://doi.org/10.1016/S0168-9002(03)01368-8)
- [21] R. Brun and F. Rademakers, “ROOT: An object oriented data analysis framework”, *Nucl. Instrum. Meth. A*, vol. 389, pp. 81–86, 1997.  
[doi:10.1016/S0168-9002\(97\)00048-X](https://doi.org/10.1016/S0168-9002(97)00048-X)
- [22] S. Navas, C. Amsler, T. Gutsche, C. Hanhart, J. J. Hernández-Rey, C. Lourenço, *et al.*, “Review of particle physics”, *Phys. Rev. D*, vol. 110, no. 3, p. 030001, Aug. 2024.  
[doi:10.1103/PhysRevD.110.030001](https://doi.org/10.1103/PhysRevD.110.030001)